Journal of
Nanoscience and Nanotechnology
Vol. 13, 7982–7987, 2013

RESEARCH ARTICLE

Origin of the Mixing Ratio Dependence of Power Conversion Efficiency in Bulk Heterojunction Organic Solar Cells with Low Donor Concentration

Hyung-Jun Song[1], Jun Young Kim[1], Donggu Lee[1], Jiyun Song[1], Youngjun Ko[1], Jeonghun Kwak[2], and Changhee Lee[1,*]

[1] *Department of Electrical and Computer Engineering, Global Frontier Center for Multiscale Energy Systems, Seoul National University, Seoul 151-742, Republic of Korea*
[2] *Department of Electronic Engineering, Dong-A University, Busan 604-714, Republic of Korea*

We studied the origin of the improvement in device performance of thermally evaporated bulk heterojunction organic photovoltaic devices (OPVs) with low donor concentration. Samples with three different donor–acceptor mixing ratios, 0:10 (C_{70}-only), 1:9 (low-doped) and 3:7 (high-doped), were fabricated with 1,1-bis-(4-bis(4-methyl-phenyl)-amino-phenyl)-cyclohexane (TAPC):C_{70}. The power conversion efficiencies (PCEs) of these samples were 1.14%, 2.74% and 0.69%, respectively. To determine why the low-doped device showed a high PCE, we measured various properties of the devices in terms of the effective energy band gap, activation energy, charge carrier mobility and recombination loss. We found that the activation energy for charge carrier transport was increased as we increased the TAPC concentration in the blends whereas the hole and electron mobilities became more balanced as the TAPC concentration was increased. Furthermore, the recombination loss parameter α (from the light intensity dependence) remained $\alpha \sim 0.9$ in the low-doped device, but it decreased to $\alpha \sim 0.77$ in the high-doped device, indicating a large recombination loss as a result of space charge. Therefore, the improved PCE of low-doped OPVs can be attributed to the balance between carrier mobilities with no increase in recombination loss.

Keywords: Organic Photovoltaic Cells, Small Molecule, Bulk Heterojunction, Donor–Acceptor Mixing Ratio.

1. INTRODUCTION

Thermally evaporated small-molecule-based organic photovoltaic cells (OPVs) have received considerable attention because of their advantages over their polymeric counterparts such as high purity, well-ordered film structure and uniform performance without batch-to-batch variation.[1,2] In terms of device structure, bulk heterojunction (BHJ) OPVs, based on a network of donor and acceptor molecules in the active layer, are widely used because of their remarkably high power conversion efficiency (PCE).[3] To increase the performance of BHJ-OPVs, many efforts have been made, such as an alternative thermal deposition technique, substrate heating a post-annealing process and adding co-evaporant molecules.[4–7]

Recently, Tang et al. reported that BHJ-OPVs with a low ratio of donor molecules led to an enhancement in the PCE by dramatically increasing the photocurrent.[8] By contrast, it has been shown that the PCE of devices whose donor concentration exceeds the proper ratio decreases sharply. Thus, it is necessary to understand how donor molecules behave in BHJ-OPVs as a function of their concentration. However, to date, donor molecules have simply been considered paths for hole carriers and the influence of them on electrical properties of devices have not been studied. Furthermore, the origin of the decrease in the PCE in devices with high donor concentrations has not been clearly elucidated.

In this study, we analyzed the origin of the donor concentration dependence of PCE in low-donor-doped BHJ-OPVs by measuring the electrical characteristics of the devices at different temperatures. The results show that improving carrier mobility without affecting recombination loss in low-donor-doped devices leads to an enhancement in the PCE.

*Author to whom correspondence should be addressed.

 1533-4880/2013/13/7982/006 doi:10.1166/jnn.2013.8155

2. EXPERIMENTAL DETAILS

The device structure employed in this study is illustrated in Figure 1(a). Devices were fabricated on cleaned indium-tin oxide (ITO)-coated glass substrates. For hole extraction and to make a Schottky contact with the active layer, 5-nm molybdenum oxide (MoO_3) and 3-nm 1,1 bis-(4-bis(4-methyl-phenyl)-amino-phenyl)-cyclohexane (TAPC) layers were sequentially deposited.[9, 10] An active layer with a thickness of 45 nm was formed by co-evaporating an acceptor material, C_{70} (Electrical Materials Index Corp.), and a donor material, TAPC (Luminescence Technology Corp.). To verify the effect of the donor–acceptor mixing ratio on OPVs, three samples with different TAPC concentrations were prepared. The active layer of the first one was pure C_{70} (C_{70}-only). The second one contained 10% (volume ratio) TAPC relative to the C_{70} content (low-doped). The donor concentration of the third device was 30% (high-doped). Before evaporating a lithium fluoride (LiF)/aluminum (Al) cathode, a 10-nm 4,7-diphenyl-1,10-phenanthroline (Bphen) layer was inserted to block hole carriers.[11] The evaporation rate of C_{70} was fixed at 1 Å/s for all samples, but that of TAPC ranged from 0.1 Å/s (low-doped) to 0.3 Å/s (high-doped) using two independently controlled heating sources. The rates of deposition for MoO_3, TAPC buffer, Bphen, LiF and Al were 1, 0.5, 1, 0.05 and 3 Å/s, respectively. All samples were fabricated in a high-vacuum system ($< 5 \times 10^{-6}$ Torr) and encapsulated in an argon atmosphere to prevent the devices from degradation. The size of the devices was 20 mm^2.

To measure the carrier mobility single-carrier devices were also fabricated. To eliminate the side effects from different injection layers, the buffer layers in the devices were the same as those used in OPVs. In electron-only devices, Al was used for both electrodes to match the work function with the lowest unoccupied molecular orbital (LUMO) level of C_{70}.[12, 13] Moreover, 10-nm Bphen layers were inserted between the 100-nm C_{70}:TAPC layer and both electrodes to prevent hole injection from the electrodes. In contrast, the electrodes typically used for hole-only devices were ITO and gold, whose work functions are higher than the work function of Al.[12] Additionally, 10-nm MoO_3 layers were used as hole buffers to make an ohmic contact. The deposition rates and TAPC doping ratio for the single-carrier devices were the same as those used in the OPVs.

The photocurrent–voltage characteristics of the cells were measured at temperatures ranging from 100 K to 400 K in the dark and under irradiation intensities ranging from 2 mW/cm^2 to 100 mW/cm^2 using a solar simulator (Newport 91160A, Air mass (AM) 1.5 G with a KG 5 filter). All measurements were taken under low vacuum by using a Keithley 237 source measurement unit.

3. RESULTS AND DISCUSSION

3.1. Effective Energy Gap

The current density–voltage curves for the three devices with different donor–acceptor mixing ratios at room temperature are shown in Figure 1(b). The PCEs of the C_{70}-only, low-doped and high-doped samples were 1.14%, 2.74% and 0.69%, respectively. The PCE of the low-doped device was much higher than the PCE of the other devices, which is consistent with the results of a previous study.[8] To investigate the main sources of improvement in the PCE, we measured the OPV characteristics in terms of the open-circuit voltage (V_{OC}), short-circuit current density (J_{SC}), fill factor (FF) and PCE by changing the device temperature.

The temperature dependence of V_{OC} is depicted in Figure 2(a). The V_{OC} of all devices decreased linearly with increasing temperature, as indicated by the following equation for a p–n junction solar cell,[14]

$$V_{OC} = \frac{E_g}{e} - C\frac{k_B T}{e} \quad (1)$$

where E_g is the energy band gap between the LUMO of an acceptor and the highest occupied molecular orbital (HOMO) of a donor, C is a constant, k_B is the Boltzmann

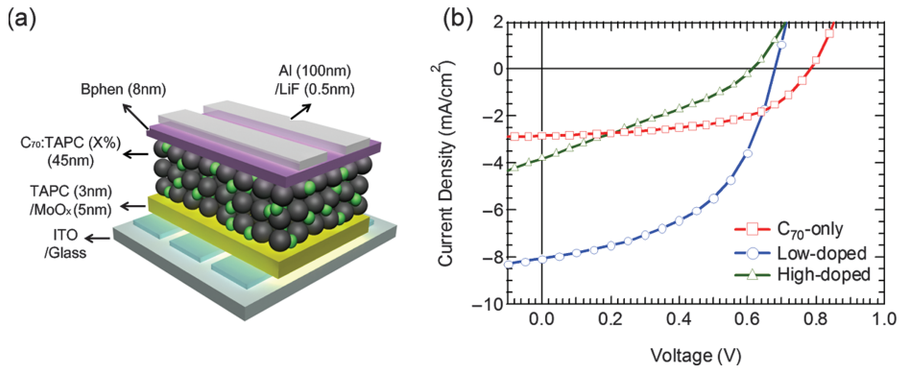

Fig. 1. (a) Schematic of the device structure and (b) current density–voltage characteristics under a light intensity of 100 mW/cm^2 for OPVs with different donor ratios.

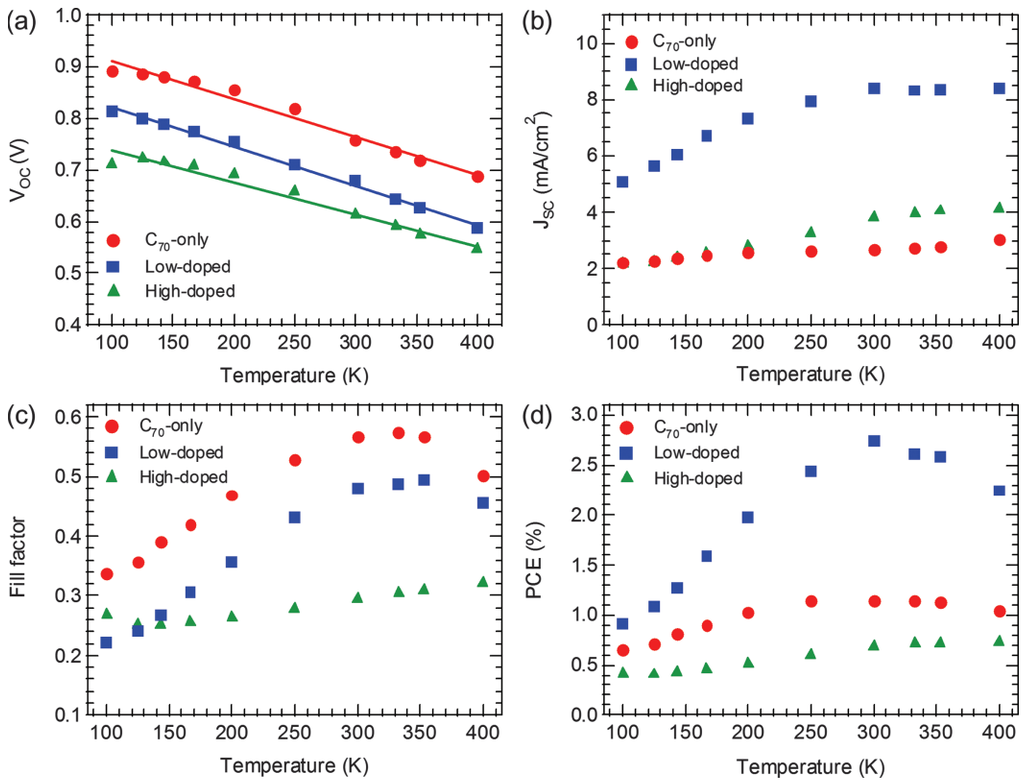

Fig. 2. Photovoltaic performance parameters in terms of (a) V_{OC}, (b) J_{SC}, (c) FF and (d) PCE for C_{70}-only, low-doped and high-doped devices as a function of absolute temperature under a light intensity of 100 mW/cm^2. The solid line in (a) represents the fit using Eq. (1).

constant, T is the absolute temperature and e is the charge of a single electron. However, in this case, the effective E_g can be considered the energy band gap between the HOMO of the buffer layer and the LUMO of the active layer because the donor doping ratio is sufficiently low.[8] The effective E_g values, deduced from Eq. (1), for the C_{70}-only, low-doped and high-doped cells were 0.98 eV, 0.90 eV and 0.80 eV, respectively. These values indicate that the effective E_g decreased with the increasing concentration of donor molecules in the composite. Because the HOMO of the TAPC buffer layer was fixed, the decrease in the effective E_g originated from the drop in the effective LUMO level of the active layer. As a result, the V_{OC} decreased as the donor concentration increased.[15] However the variation in V_{OC} is not sufficiently large to explain the drastic decrease in the PCE of the high-doped device and contradicts the improvement in the PCE of the low-doped device. Hence, the V_{OC} is negatively correlated with the donor concentration due to the change in the effective E_g though the change in the V_{OC} has limited effects on the PCE.

3.2. Activation Energy

By contrast, as shown in Figures 2(b) and (c), as the temperature was increased, a substantial enhancement in J_{SC} and FF was observed in the low-doped device compared to the high-doped device. The change in these two factors, J_{SC} and FF, is mainly attributable to the variation in the PCE (see Fig. 2(d)).

In the C_{70}-only and low-doped devices, the PCE showed a negative parabolic dependence on temperature, which was optimized at room temperature, analogous to the temperature dependence of FF. In disordered organic films, it is well known that this shape is due to the combination of two factors: an improvement in carrier transport by hopping as the temperature increases and a decrease in mobility due to phonon scattering at much higher temperatures.[16, 17] This temperature dependence indicates that carriers can be easily extracted by the electrodes of these devices at room temperature. By contrast, in the high-doped device, the PCE as well as the FF and J_{SC} were continuously improved as the temperature increased up to 400 K, which indicates that high thermal energy helped release carriers held in trap sites. Thus, the donor concentration is correlated with the energy depth of trap sites.

To determine the energy level of traps, ln J_{SC} versus inverse temperature (1000/T) under different light intensities was measured, as shown in Figure 3. According to the Arrhenius equation, J_{SC} can be expressed as a function of temperature, light intensity and activation energy (AE, Δ),

$$J_{SC}(T, P_{Light}) = J_0(P_{Light}) \times \exp\left(-\frac{\Delta}{k_B T}\right) \quad (2)$$

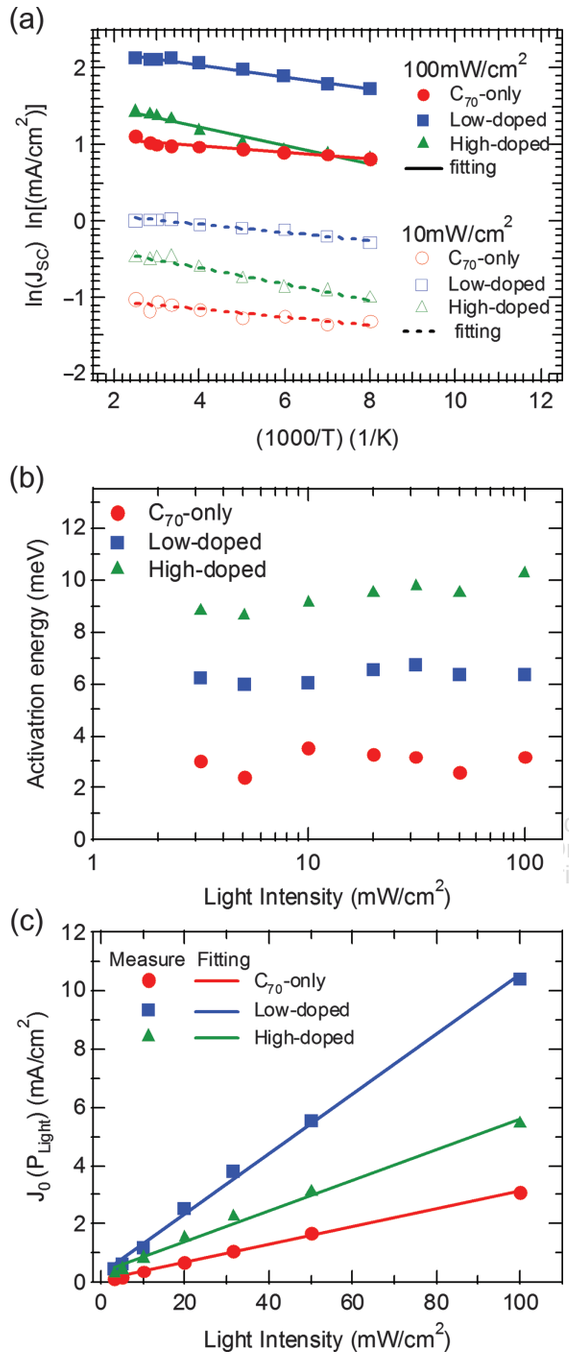

Fig. 3. (a) Arrhenius equation plots of ln J_{SC} versus the inverse absolute temperature under different incident light intensities of 10 mW/cm^2 (open) and 100 mW/cm^2 (closed). The solid fitting lines are for 100 mW/cm^2 and the dotted ones for 10 mW/cm^2. (b) The activation energy and (c) the pre-exponential factor for OPVs with different donor: acceptor ratios.

where P_{Light} is the incident light intensity.[18] The term $J_0(P_{Light})$ reflects the amount of photocurrent associated with carrier mobility, the number of carriers and electrical field, while the exponential term represents the energy depth of traps.[18, 19]

The AE for the high-doped (8.6–10.3 meV) device was higher than that for the C_{70}-only (2.5–3.5 meV) and low-doped (5.9–6.7 meV) devices at each light intensity, as shown in Figure 3(b). The AE increased in proportion to the concentration of donor molecules in the blend layer. The AE values for the low-doped and the C_{70}-only devices were not sufficiently high to allow carriers to easily move to the electrode with small losses in energy, while the AE for the high-doped device was quite high, preventing captured carriers from easily overcoming the energy barrier. In other words, donor molecules act as trap sites that hinder the transport of carriers to electrodes; thus, the high AE led to a decrease in the PCE of the highly doped OPVs.

3.3. Carrier Mobility

The pre-exponential factor $[J_0(P_{Light})]$ in the Arrhenius equation also supports the enhancement in the PCE of the low-doped device, as illustrated in Figure 3(c). As mentioned previously, the factor is governed by two electrical properties: carrier mobility and the number of carriers that are involved in recombination. Thus, we investigated the relationship between these two factors and the donor concentration.

First, Figure 4 shows the hole and electron mobility as a function of the TAPC ratio in the single-carrier devices. The mobility was obtained by considering a space-charge-limited current model under an electric field of 1×10^5 V/cm. The hole mobility of the low-doped device (2.8×10^{-6} cm^2/V · s) was one order of magnitude higher than that of the pure C_{70} film (2.7×10^{-7} cm^2/V · s), while the value of the high-doped device (4.6×10^{-6} cm^2/V · s) did not significantly increase beyond that of the low-doped one. Similar results were previously reported for OPVs based on fullerene derivative/polymer blends or vacuum-evaporated C_{60}/donor mixtures.[20, 21]

Meanwhile, the electron mobility of the devices remained within the same order of magnitude, even though the donor concentration reached up to 30%. The electron mobility for the low-doped (3.9×10^{-3} cm^2/V · s)

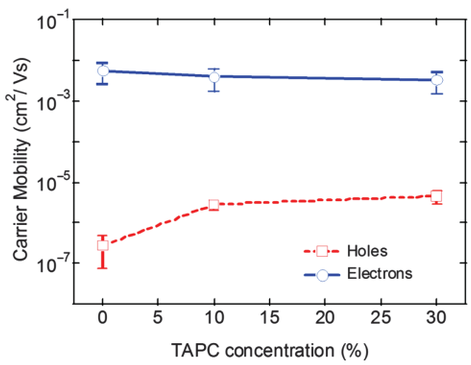

Fig. 4. Hole and electron mobility of single-carrier devices as a function of TAPC concentration. The error bars indicate the deviation among samples with the same doping ratio.

Table I. Electrical properties of OPVs with different donor concentrations.

	C_{70}-only	Low-doped	High-doped
Effective E_g (eV)	0.98	0.90	0.80
AE (meV)	2.5–3.5	5.9–6.7	8.6–10.3
Hole mobility (cm^2/Vs)	2.7×10^{-7}	2.8×10^{-6}	4.6×10^{-6}
Electron mobility (cm^2/Vs)	5.6×10^{3}	3.9×10^{3}	3.2×10^{3}
α	0.90–0.91	0.90	0.77–0.84

and high-doped (3.2×10^{-3} $cm^2/V \cdot s$) films did not vary much compared with that of the neat C_{70} layer (5.6×10^{-3} $cm^2/V \cdot s$). This result is in agreement with that of a previous study, in which the electron mobility remained nearly the same until donor molecules were added to BHJ blends in concentrations of up to 30%.[12, 13] Moreover, doping reduced the gap between the electron and the hole mobility by enhancing hole transport. This balanced mobility between electron and hole transport consequently improved the values of the pre-exponential factor in doped devices, resulting in the improvement of the PCE.[22]

3.4. Recombination Loss

To probe the recombination characteristics that also affect the pre-exponential value, J_{SC} values were measured under light intensities ranging from 2 mW/cm^2 to 100 mW/cm^2. Figure 5 shows the light-intensity dependence of J_{SC} ($J_{SC} = P_{Light}^{\alpha}$) for devices on a double-logarithmic scale. Here, α is a power-law value that represents recombination properties. Several authors have reported that monomolecular recombination dominates the recombination properties of a device when α is close to 1. Meanwhile, when $\alpha = 0.75$, the recombination loss of a device is controlled by space charges.[23–25] The α of the C_{70}-only and low-doped devices ranges from 0.90 to 0.91 throughout the entire range of temperatures, whereas the value of the high-doped one increases from 0.77 ($T = 100$ K) to 0.84 ($T = 400$ K). Therefore, the C_{70}-only and low-doped devices are in the monomolecular recombination region and the high-doped device is close to the space-charge limited recombination state.

The reduction in the photocurrent of a device in the monomolecular recombination region is generally smaller than that due to space charges because photo-generated carriers are quenched only by intrinsic impurities in this region. Thus, the recombination loss in the C_{70}-only and low-doped OPVs was low, while the high-doped one exhibited a high space-charge-limited recombination loss due to deep-trapped charges. The temperature dependence of α in the high-doped cell can also be understood by considering these captured carriers, which had a higher probability of being released from trapped states at high temperature. Thus, not only J_{SC} but also FF decreased in the high-doped cell because the free-charge extraction efficiency was suppressed by the recombination loss.[26] Therefore, the small recombination loss in the low-doped device improved J_{SC} and FF, while the mobility-balanced state in the high-doped sample was overwhelmed by recombination loss.

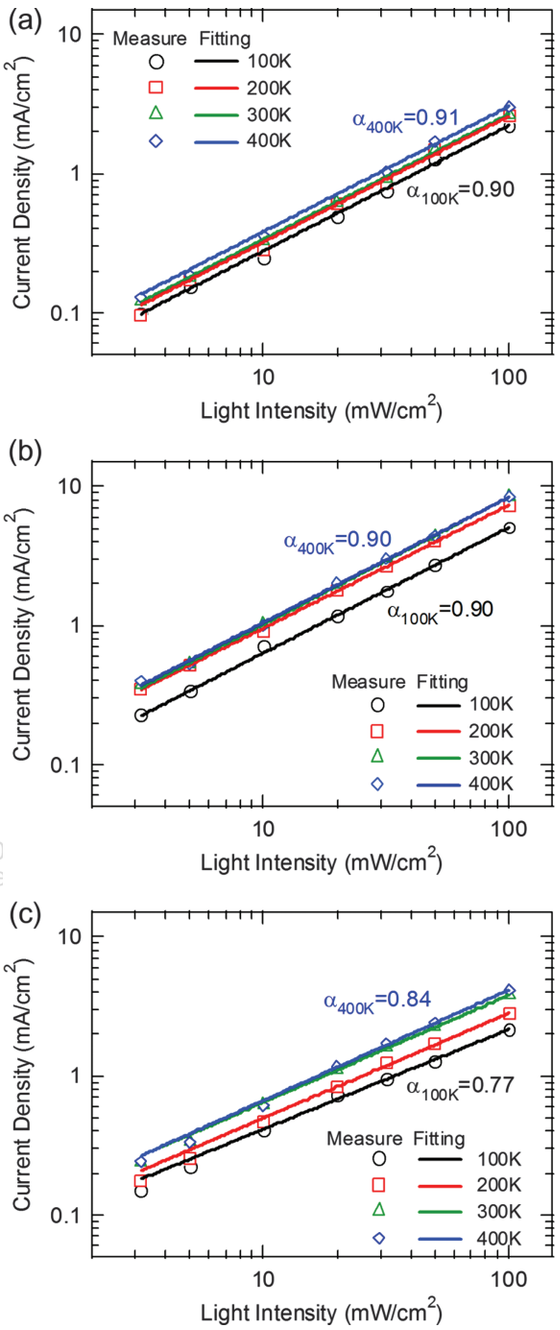

Fig. 5. The J_{SC} under different light intensities for (a) C_{70}-only, (b) low-doped and (c) high-doped devices at different temperatures. The power-law-dependent factor α at 100 K and 400 K is marked in each graph.

4. CONCLUSIONS

In summary, we investigated the effect of donor doping on BHJ-OPVs to assess the origin of PCE enhancement

in low-doped cells. The doping of donor molecules in the active layer influenced four electrical properties of the devices: the effective E_g, activation energy, carrier mobility and recombination loss. Although donor doping reduced the effective E_g and produced trap sites, the photocurrent increased owing to the facilitation of hole carrier transport by a small activation energy and balanced electron–hole mobility in the low-doped device. Furthermore, at small doping ratios, the recombination loss was not increased. Therefore, we can conclude that these factors are important in developing highly efficient OPVs. We also believe that the analysis and results reported in this paper will aid in developing and further improving other small-molecule-based BHJ-OPVs.

Acknowledgments: This work was supported by the Human Resources Development Program of the Korea Institute of Energy Technology Evaluation and Planning (KETEP) grant funded by the Korea government Ministry of Knowledge Economy (No. 20124010203170).

References and Notes

1. B. Walker, A. B. Tamayo, X.-D. Dang, P. Zalar, J. H. Seo, A. Garcia, M. Tantiwiwat, and T.-Q. Nguyen, *Adv. Funct. Mater.* 19, 3063 (**2009**).
2. A. Mishra and P. Bäuerle, *Angew. Chem. Int. Ed.* 51, 2020 (**2012**).
3. C. J. Brabec, N. S. Sariciftci, and J. C. Hummelen, *Adv. Funct. Mater.* 11, 15 (**2001**).
4. J. W. Kim, H. J. Kim, H. H. Lee, T. Kim, and J.-J. Kim, *Adv. Funct. Mater.* 21, 2067 (**2011**).
5. D. Wynands, M. Levichkova, M. Riede, M. Pfeiffer, P. Baeuerle, R. Rentenberger, P. Denner, and K. Leo, *J. Appl. Phys.* 107, 014517 (**2010**).
6. J. Y. Kim, J. Kwak, S. Noh, and C. Lee, *J. Nanosci. Nanotechnol.* 12, 5724 (**2012**).
7. T. Kaji, M. Zhang, S. Nakao, K. Iketaki, K. Yokoyama, C. W. Tang, and M. Hiramoto, *Adv. Mater.* 23, 3320 (**2011**).
8. M. Zhang, H. Wang, H. Tian, Y. Geng, and C. W. Tang, *Adv. Mater.* 23, 4960 (**2011**).
9. Irfan, M. Zhang, H. Ding, C. W. Tang, and Y. Gao, *Org. Electron.* 12, 1588 (**2011**).
10. P. M. Borsenberger, L. Pautmeier, R. Richert, and H. Bässler, *J. Chem. Phys.* 94, 8276 (**1991**).
11. S. Naka, H. Okada, H. Onnagawa, and T. Tsutsui, *Appl. Phys. Lett.* 76, 197 (**2000**).
12. R. Pandey, A. A. Gunawan, K. A. Mkhoyan, and R. J. Holmes, *Adv. Funct. Mater.* 22, 617 (**2012**).
13. V. D. Mihailetchi, L. J. A. Koster, P. W. M. Blom, C. Melzer, B. de Boer, J. K. J. van Duren, and R. A. J. Janssen, *Adv. Funct. Mater.* 15, 795 (**2005**).
14. M. D. Perez, C. Borek, S. R. Forrest, and M. E. Thompson, *J. Am. Chem. Soc.* 131, 9281 (**2009**).
15. G. Chen, H. Sasabe, Z. Wang, X. F. Wang, Z. Hong, Y. Yang, and J. Kido, *Adv. Mater* 24, 2768 (**2012**).
16. D. Chirvase, Z. Chiguvare, M. Knipper, J. Parisi, V. Dyakonov, and J. C. Hummelen, *J. Appl. Phys.* 93, 3376 (**2003**).
17. P. M. Borsenberger, L. Pautmeier, and H. Bässler, *J. Chem. Phys.* 94, 5447 (**1991**).
18. I. Riedel and V. Dyakonov, *Phys. Stat. Sol.* (*a*) 201, 1332 (**2004**).
19. J. Schafferhans, C. Deibel, and V. Dyakonov, *Adv. Ener. Mater.* 1, 655 (**2011**).
20. A. Opitz, M. Brönner, J. Wagner, M. Götzenbrugger, and W. Brütting, *Proc. SPIE* 7002, 70020J (**2008**).
21. S. M. Tuladhar, D. Poplavskyy, S. A. Choulis, J. R. Durrant, D. D. C. Bradley, and J. Nelson, *Adv. Funct. Mater.* 15, 1171 (**2005**).
22. J. H. Seo, J.-R. Koo, S. J. Lee, B. M. Seo, and Y. K. Kim, *J. Nanosci. Nanotechnol.* 11, 7307 (**2011**).
23. L. J. A. Koster, V. D. Mihailetchi, H. Xie, and P. W. M. Blom, *Appl. Phys. Lett.* 87, 203502 (**2005**).
24. V. D. Mihailetchi, J. Wildeman, and P. W. M. Blom, *Phys. Rev. Lett.* 94, 126602 (**2005**).
25. P. Schilinsky, C. Waldauf, and C. J. Brabec, *Appl. Phys. Lett.* 81, 3885 (**2002**).
26. R. Mauer, I. A. Howard, and F. Laquai, *J. Phys. Chem. Lett.* 1, 3500 (**2010**).

Received: 1 May 2012. Accepted: 20 December 2012.

RESEARCH ARTICLE